Hindawi Publishing Corporation
International Journal of Antennas and Propagation
Volume 2014, Article ID 701279, 6 pages
http://dx.doi.org/10.1155/2014/701279

Research Article

A Miniaturized Frequency Selective Surface Based on Square Loop Aperture Element

Wenxing Li,[1] Chunming Wang,[1] Yong Zhang,[2] and Yingsong Li[1]

[1] *College of Information and Communications Engineering, Harbin Engineering University, Harbin, Heilongjiang 150001, China*
[2] *DEEHOW Electronics Technology Co., Ltd., Beijing 100043, China*

Correspondence should be addressed to Chunming Wang; wangchunming@hrbeu.edu.cn

Received 19 January 2014; Accepted 24 February 2014; Published 27 March 2014

Academic Editor: Wenhua Yu

Copyright © 2014 Wenxing Li et al. This is an open access article distributed under the Creative Commons Attribution License, which permits unrestricted use, distribution, and reproduction in any medium, provided the original work is properly cited.

We propose a miniaturized band-pass frequency selective surface (FSS) with periodic unit cell structure. The proposed FSS is realized by symmetrically bending the edges of the square loop aperture element, by which our proposed FSS increases the resonant length, and, hence, reduces its size. In this FSS, each unit cell has a dimension of $0.0538\lambda \times 0.0538\lambda$, where λ represents the wavelength of the corresponding resonant frequency. Both the theoretical analysis and simulation results demonstrate that our proposed FSS, having high polarization stability and angle stability, can achieve smaller size in comparison with the previously proposed structures.

1. Introduction

Frequency selective surfaces (FSSs) are two-dimensional planar periodic structures which are realized by using patch or aperture elements to provide frequency filtering characteristic to incoming wave [1]. FSS has attracted a great amount of attention and has been widely studied for microwave and light-wave applications owing to its frequency selective properties [1–7]. Recently, FSS has been adopted in subreflector of Cassegrain antenna system to achieve frequency reuse, used to design band-pass radomes on the aircraft to reduce the out-of-band radar cross section (RCS) of antennas, and used in circuit analog absorber to expand its bandwidth [2].

FSS is an infinite periodic array, which is difficult to design. In fact, it can be implemented by using finite elements to make it suitable for practical engineering applications. This is because the finite FSS structure has no infinite expansibility and results in end current and scattering at the edges of the finite array, which seriously affect the performance of the FSS [3]. Therefore, it is necessary to use sufficient elements to approximate the characteristics of infinite FSS. Generally, the number of unit cells should not be less than 20×20 [4]. However, the size of a unit cell is so large that it is difficult to design a finite FSS array with sufficient number of elements in a finite space when the FSS is operating in a low frequency such as L-band. As a result, minimization of FSS becomes one of the attractive and hot topics. Furthermore, the FSS should have good resonance stability performance with respect to various polarizations and incidence angles to achieve stable filter property in operating band [5].

Recently, a great number of FSSs have been developed to reduce their sizes. Chiu and Chang proposed a novel FSS structure which is realized by using two metal patch layers and a dielectric layer. The two metal patch layers coupled together via the dielectric layer. The size of each element is $0.104\lambda \times 0.104\lambda$ [5]. Then, Li et al. developed an octagon FSS using fractal theory and reduced the final FSS element size to $0.0814\lambda \times 0.0814\lambda$ [6]. After that, Yang et al. reported an improved FSS by bending the edges of cross aperture element into the external space [7] and the size of each element was $0.061\lambda \times 0.061\lambda$. All these unit cells are symmetrical in order to ensure the stability of the corresponding FSSs. However, the size of the FSS is still large for practical applications in very low frequency.

In this paper, we propose a miniaturized band-pass FSS with periodic unit cell structure. The proposed FSS is realized by symmetrically bending the edges of the square loop aperture element to the inner space. In this FSS, each unit

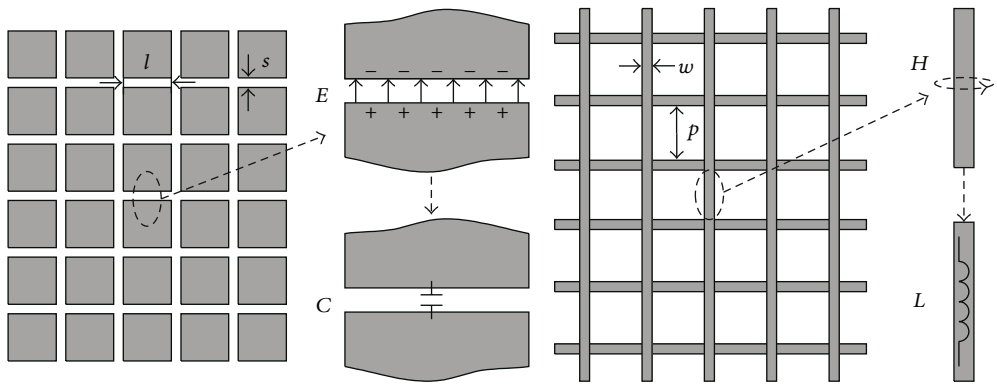

(a) Equivalent capacitance of patch array (b) Equivalent inductance of wire grid

Figure 1: Equivalent analysis of periodic structure.

cell has a dimension of $0.0538\lambda \times 0.0538\lambda$. The simulation results demonstrate that our proposed FSS, having high polarization stability and angle stability, can achieve smaller size in comparison with the previously proposed structures.

2. Fundamental of Miniaturized FSS

On the basis of the electromagnetic theory, when a plane wave is incident on a patch array, there exists induced current. Examples are shown in Figure 1. In Figure 1(a), we choose the vertical direction as reference direction of electric field in the two-dimensional plane. When a plane wave is incident on a patch array, the electric field creates positive and negative charges on the edges of the two adjacent patches, which is a gap capacitor. Similarly, in a wire grid shown in Figure 1(b), parallel wires can also generate induced current, resulting in a magnetic field, which acts as inductors. The first-order approximation of the capacitance of the patch array and the inductance of a wire gird are determined by (1) and (2), respectively [8]:

$$C = \varepsilon_0 \varepsilon_{\text{eff}} \left(\frac{2l}{\pi}\right) \log\left[\csc\left(\frac{\pi s}{2l}\right)\right], \quad l > s, \tag{1}$$

$$L = \mu_0 \left(\frac{p}{2\pi}\right) \log\left[\csc\left(\frac{\pi w}{2p}\right)\right], \quad p > w, \tag{2}$$

where ε_0 is the permittivity constant of the air, ε_{eff} is the effective dielectric constant of the substrate, l is the side length of the patches, s is the distance between the two patches, μ_0 is the permeability of air, p is the length of the wire, and w is the width of the wire.

From (1), we find that C is proportional to l and is inversely proportional to s when $l > s$. In a word, only the narrow apertures in the horizontal direction act as big equivalent capacitance, which is shown in Figure 1(a). In (2), we observe that L is proportional to p and is inversely proportional to w with $p > w$. Thus, the equivalent inductance effects are mainly dependent on the vertical direction of these long wires.

Based on the theoretical analysis and discussions above, we can choose appropriate dimensions of the FSS elements to obtain required resonant frequency. In addition, we know that different FSS structures may have different equivalent circuits. For square loop aperture element illustrated in Figure 2, the narrow aperture in horizontal direction plays an important role in forming the big equivalent capacitance, the long wire in vertical direction plays an important role in forming the big equivalent inductance [2], and the equivalent circuit model of such element is shown in Figure 3, in which C is large equivalent capacitance and L is large equivalent inductance.

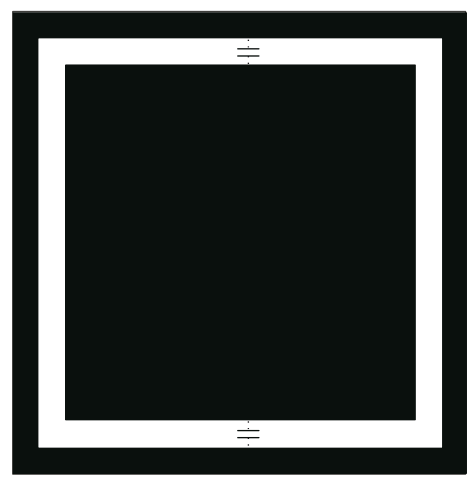

Figure 2: Square loop aperture element.

From the previous knowledge on the circuit analysis, the resonant frequency of the equivalent model described in Figure 3 can be expressed as

$$f = \frac{1}{\left(2\pi\sqrt{L_s C_s}\right)}, \tag{3}$$

where $C_s = 0.5C$ and $L_s = 0.5L$.

From (1), (2), and (3), we find that the resonant frequency of the square loop aperture element mainly relies on the equivalent capacitance C and the equivalent inductance L. As for the square loop aperture FSS, we should increase the

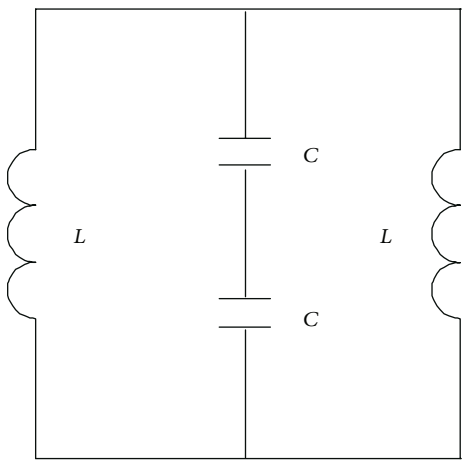

Figure 3: Equivalent model of square loop aperture element.

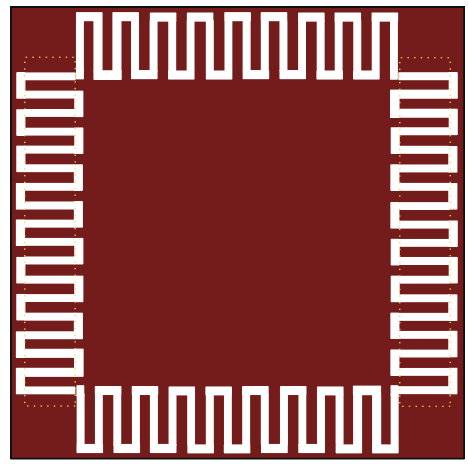

Figure 4: Structure of FSLA element.

Table 1: Parameters of the designed FSS element.

Parameter	Value
Length (D)	9.8 mm
Width of the narrow aperture (w_1)	0.2 mm
Space between the aperture strips (w_2)	0.2 mm
Aperture space of adjacent elements (g)	0.2 mm
Thickness of the metal layer (t)	0.2 mm
Thickness of the dielectric layer (h)	1.6 mm
Loss tangent of the dielectric ($\tan\theta$)	0.025
Relative dielectric constant (ε_r)	5.0

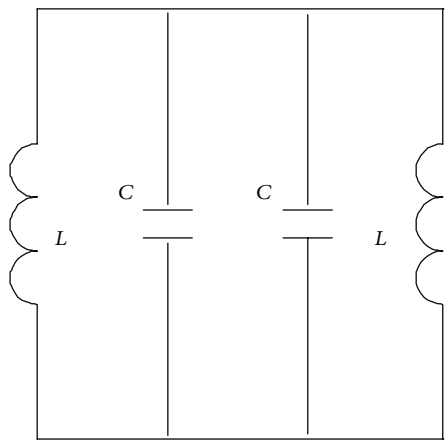

Figure 5: Equivalent model of FSLA element.

length of the narrow aperture of the element structure to obtain large equivalent capacitance so as to reduce the size of the FSS structure. Inspired by the analysis given above, we propose an improved unit cell structure named four sides loading aperture (FSLA) element, and it is shown in Figure 4. In this structure, the apertures implied by the yellow dotted line can act as large capacitors. The corresponding equivalent circuit model is shown in Figure 5, where C is the large equivalent capacitance and L is the large equivalent inductance.

To further reduce the resonant frequency of the above structure, we bend the FSLA element into the inner side of the square loop. The new structure of the highly improved FSS unit cell is described in Figure 6 and its equivalent model can also be illustrated by using the model shown in Figure 5. However, the values of the two capacitances in Figure 5 increase.

3. Results and Discussions

On the basis of the analysis, we propose a miniaturized FSS, which operates at 1.647 GHz. The FSS element is shown in Figure 6 while the related parameters are shown in Table 1.

The simulation results are obtained by using the computer simulation technology (CST). The simulated model is shown in Figure 7 and the transmission coefficients with normal incidence of the designed FSS are shown in Figure 8. We can see from Figure 8 that the resonant frequency of our designed FSS is 1.647 GHz for normal incidence. When ε_r is 2.65, the resonant frequency is 1.995 GHz; when ε_r is 4.4, the resonant frequency is 1.713 GHz.

According to the results shown in Figure 8 and (4), the size of the FSS element can be obtained with size of $0.0538\lambda \times 0.0538\lambda$,

$$C_0 = \lambda f,$$
$$k = \frac{D}{\lambda}, \tag{4}$$

where C_0 is the speed of light in air, f represents the resonant frequency of the FSS and λ is the corresponding wavelength, k is the size of FSS element, and D represents the length of the element.

Moreover, the element size is different as the dielectric is different. It is found that k is inversely proportional to ε_r. The proposed FSS is compared with the previously proposed studies in [5–7] and the comparisons are shown in Table 2. It can be seen from Table 2 that the designed FSS can achieve smaller size. This means that our proposed design is smaller in size at the same resonant frequency.

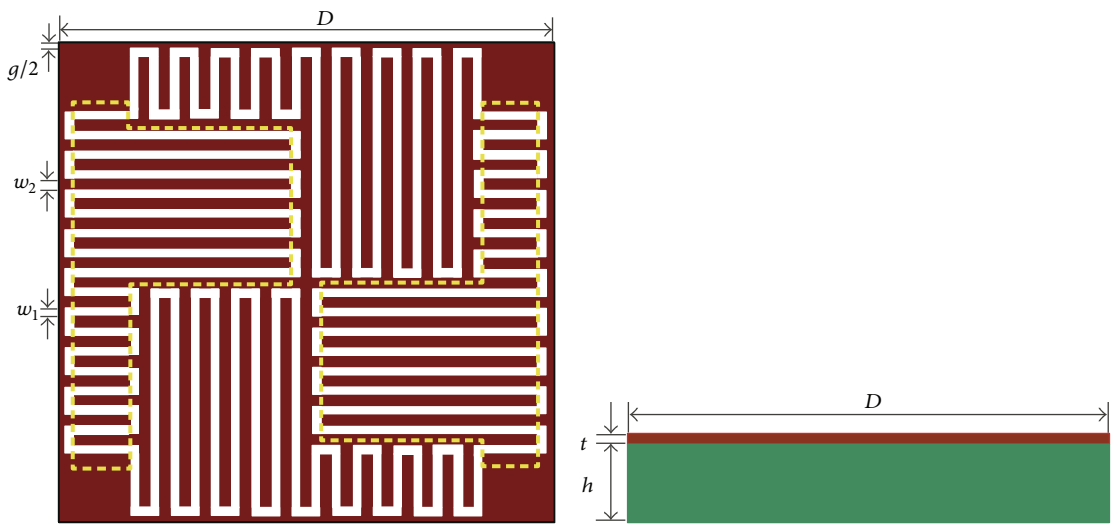

(a) Front view (b) Side view

Figure 6: Structure of the proposed FSS element.

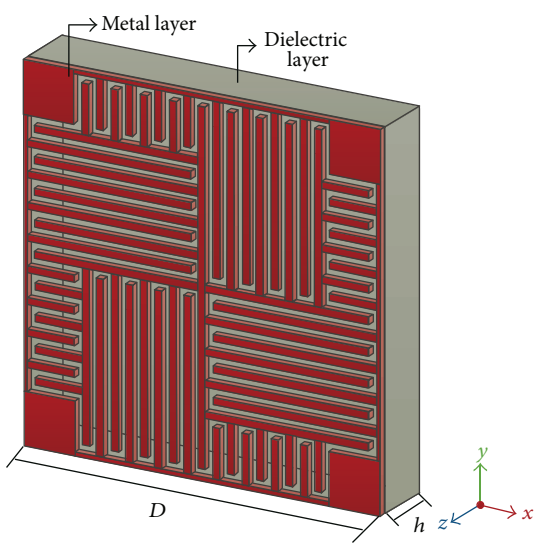

Figure 7: Simulation model of designed FSS.

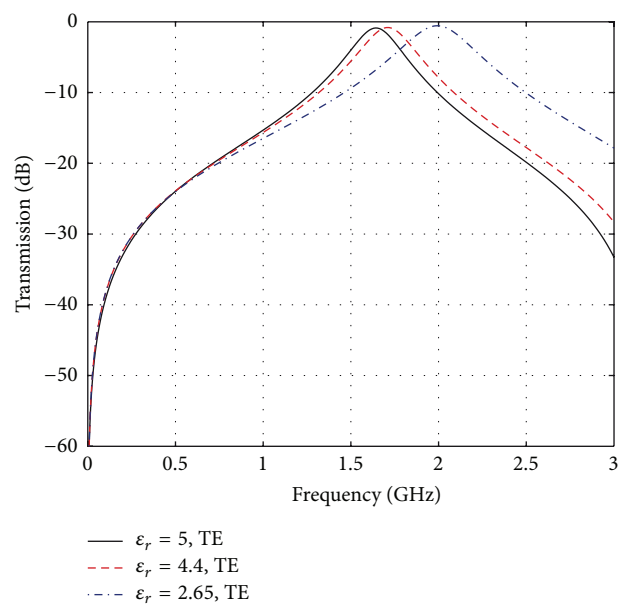

Figure 8: Transmission coefficients of designed FSS.

Table 2: Comparisons of the element sizes for the four FSSs.

FSS structure	ε_r	Element size
Paper [5]	4.4	$0.104\lambda \times 0.104\lambda$
Paper [6]	2.65	$0.0814\lambda \times 0.0814\lambda$
Paper [7]	5.0	$0.061\lambda \times 0.061\lambda$
Proposed	5.0	$0.0538\lambda \times 0.0538\lambda$
	4.4	$0.056\lambda \times 0.056\lambda$
	2.65	$0.0652\lambda \times 0.0652\lambda$

In order to further discuss the bandwidth performance of our proposed FSS, the S-parameter characteristics, including the reflection coefficient (S_{11}) and transmission coefficient (S_{21}), are obtained by using CST and the simulation results with TE-polarized incidence are shown in Figure 9. It can be seen from Figure 9 that the proposed FSS has a −10 dB impedance bandwidth of 5.34% with respect to the center frequency of 1.647 GHz.

4. Stability Analysis of the Proposed Miniaturized FSS

As a FSS, it should be stable for different applications. Therefore, we investigate the stability of the proposed miniaturized FSS for different situations, such as different polarizations or different incident angles. The simulation transmission coefficients are shown in Figure 10. As shown in Figure 10, our designed miniaturization FSS has stable resonance properties under different situations, and the resonant frequency

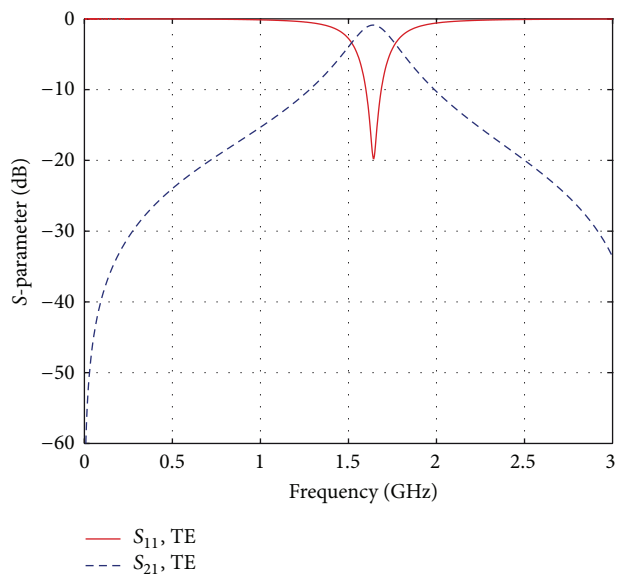

Figure 9: S-parameter characteristics of the designed FSS.

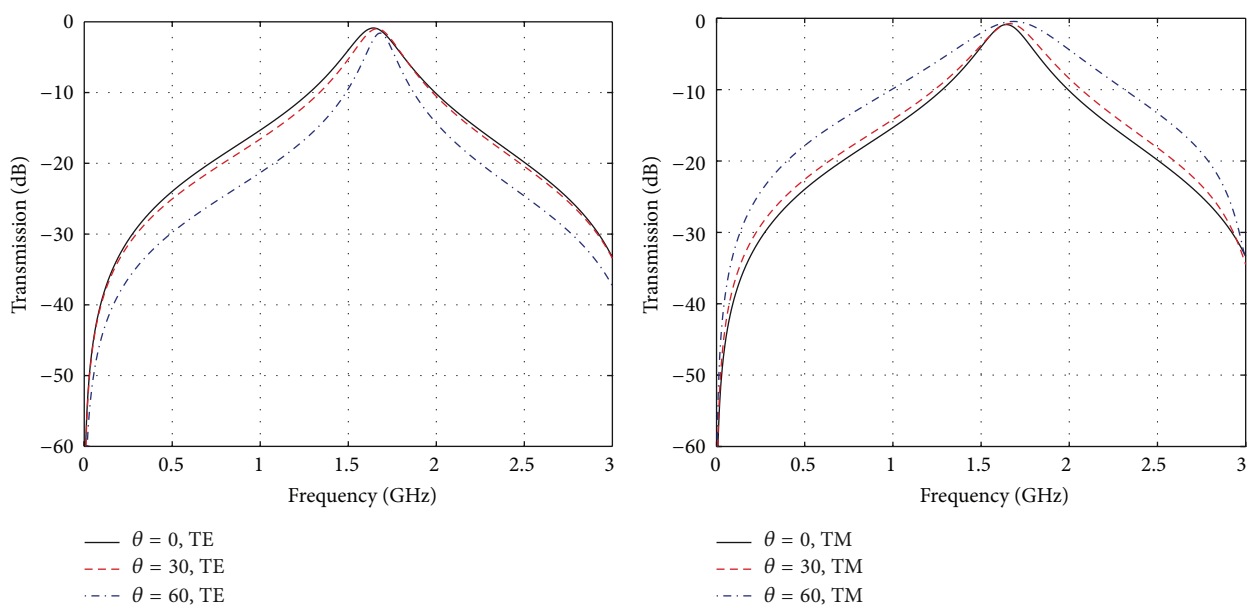

(a) TE-polarized waves with different incident angles

(b) TM-polarized waves with different incident angles

Figure 10: Transmission coefficients of the proposed miniaturized FSS with different modes.

Table 3: The resonant frequency deviation of proposed FSS at TE-polarized.

Incident angle	Resonant frequency	Deviation
$\theta = 0^\circ$	1.647 GHz	—
$\theta = 30^\circ$	1.665 GHz	1.09%
$\theta = 60^\circ$	1.683 GHz	2.19%

Table 4: The resonant frequency deviation of proposed FSS at TM-polarized.

Incident angle	Resonant frequency	Deviation
$\theta = 0^\circ$	1.647 GHz	—
$\theta = 30^\circ$	1.665 GHz	1.09%
$\theta = 60^\circ$	1.689 GHz	2.55%

deviations of the deigned miniaturization FSS are illustrated in Tables 3 and 4.

We can see from Tables 3 and 4 that the resonant frequency deviations for TE-polarized and TM-polarized

both have a little shift at different incident angles. These deviations are within the scope of the allowed operation bandwidth of the FSS. Thereby, the proposed miniaturization FSS can achieve excellent polarization stability and angle stability.

5. Conclusion

In this paper, we proposed a miniaturization FSS with unit cell size of $0.0538\lambda \times 0.0538\lambda$. The proposed FSS was designed by setting the bent FSLA element in the inner sides of the square loop. The designed FSS was analyzed step by step by using the equivalent circuit model. The simulation results obtained from CST demonstrated that our proposed FSS had excellent polarization stability and angle stability, which render it suitable for practical engineering applications.

Conflict of Interests

The authors declare that there is no conflict of interests regarding the publication of this paper.

Acknowledgments

This work was partially supported by "973" Basic Research Development Program of China (no. 6131380101). This paper is also supported by Pre-Research Fund of the 12th Five-Year Plan (no. 4010403020102) and Fundamental Research Funds for the Central Universities (HEUCFT1304).

References

[1] T. K. Wu, *Frequency Selective Surface and Grid Array*, John Wiley & Sons, New York, NY, USA, 1995.

[2] B. A. Munk, *Frequency Selective Surfaces: Theory and Design*, John Wiley & Sons, New York, NY, USA, 2005.

[3] B. A. Munk, *Finite Antenna Arrays and FSS*, John Wiley & Sons, New York, NY, USA, 2003.

[4] H.-Y. Yang, S.-X. Gong, P.-F. Zhang, F.-T. Zha, and J. Ling, "A novel miniaturized frequency selective surface with excellent center frequency stability," *Microwave and Optical Technology Letters*, vol. 51, no. 10, pp. 2513–2516, 2009.

[5] C.-N. Chiu and K.-P. Chang, "A novel miniaturized-element frequency selective surface having a stable resonance," *IEEE Antennas and Wireless Propagation Letters*, vol. 8, pp. 1175–1177, 2009.

[6] W. Li, T. Zhang, G. Yang, and Q. Wu, "A novel frequency selective surface with improved miniaturization performance," *Journal of Electromagnetic Analysis and Applications*, vol. 4, no. 3, pp. 108–111, 2012.

[7] G. Yang, T. Zhang, W. Li, and Q. Wu, "A novel stable miniaturized frequency selective surface," *IEEE Antennas and Wireless Propagation Letters*, vol. 9, pp. 1018–1021, 2010.

[8] F. Bayatpur, *Metamaterial-Inspired Frequency-Selective Surfaces*, The University of Michigan, 2009.

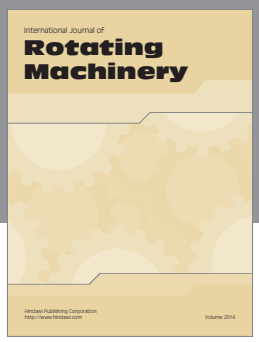

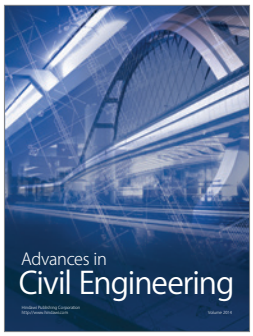

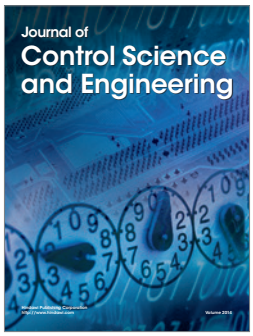

Hindawi

Submit your manuscripts at
http://www.hindawi.com